J Vis (2016) 19:631–641
DOI 10.1007/s12650-016-0363-9

REGULAR PAPER

A. Torres · M. Sánchez · F. Aragón · S. Peralta · A. Medina

Visualization of isotherms around a heated horizontal cylinder embedded in a porous medium

Received: 29 September 2015 / Revised: 25 February 2016 / Accepted: 24 March 2016 / Published online: 22 April 2016

Abstract Experiments reported here confirm experimentally the existence of the characteristic planar buoyant plumes that emerge as a consequence of the presence of a cylindrical heat source embedded in an homogeneous air-saturated and non-consolidated porous medium. The resultant buoyant plumes were visualized with IR thermography considering two important cases. First, under the action of natural convection and second, under the action of forced convection due to the passage of a constant air stream directed perpendicularly towards the horizontal cylindrical heat source buried in the porous medium. Such streams were induced at different tilt angles. For each case, the temperature distribution is shown and correspondence is found with the isotherms distribution predicted by the theoretical models reported in the literature. The use of infrared techniques appears as a helpful tool that allows us to witness all the process of rise and growth of the buoyant plumes until the phenomenon reaches steady state.

Keywords Buoyant plumes · Buoyancy-driven flows · Porous media · Heat transfer

Abbreviation

Nomenclature

a	Radius of the cylinder
g	Gravity acceleration
K	Permeability
l_h	Length scale
t_a	Diffusion time

A. Torres (✉) · S. Peralta
Instituto Mexicano del Petróleo, Eje Central Lázaro Cárdenas Norte 152, Col. San Bartolo Atepehuacan, Mexico City, CP 07730, Mexico
E-mail: war_rocket_ajax@yahoo.com.mx

M. Sánchez
ESIME Azcapotzalco, Instituto Politécnico Nacional, Av. de las granjas 682, Col. Santa Catarina, Mexico City, CP 02250, Mexico
E-mail: foxandkirvi@hotmail.com

F. Aragón
ESIME Zacatenco, Instituto Politécnico Nacional, Av. Instituto Politécnico Nacional S/N, Col. Lindavista, Mexico City, CP 07738, Mexico
E-mail: micme2003@yahoo.com.mx

A. Medina
ESIME Azcapotzalco,Instituto Politécnico Nacional, Av. de las granjas 682, Col. Santa Catarina, Mexico City, CP 02250, Mexico
E-mail: amedinao@ipn.mx

T Temperature
T_w Temperature of the cylindrical cartridge
T_∞ Room temperature
T_h Temperature scale
U_∞ Non-dimensional free stream velocity
V_h Velocity scale
V_∞ Dimensional free stream velocity
x Horizontal axis
y Vertical axis

Greek letters
α Sand effective thermal diffusivity
α_p Paperboard diffusivity
β Fluid coefficient of thermal expansion of air
γ Tilt angle referred to the positive vertical axis y
δ_p Paperboard thickness
λ Porous medium effective thermal conductivity
λ_{air} Air conductivity
λ_s Silica sand thermal conductivity
μ_f Fluid viscosity
ρ_f Fluid density
ϕ Porosity
φ Polar angle

1 Introduction

A porous medium is a material which consists of a myriad of solid grains with an interconnected void (Nield and Bejan 2013). In our work we used non-consolidated Ottawa sand which is made of spherical silica grains. This kind of internal composition allows that both the conduction and the convection phenomena can coexist. Natural convective flows induced by a constant source of heat embedded in a porous medium, merit special attention due to the interesting structures formed by the temperature gradients around the heat source. These structures are known in the literature as the buoyant plumes and they are of special interest to many engineering applications such as petroleum and geothermal reservoirs.

In the literature some theoretical approaches consider a punctual and concentrated heat source embedded in an infinite fluid-saturated porous domain. In order to describe the flow pattern and the temperature field, asymptotic solutions in terms of series expansions in the Rayleigh number (Ra) were proposed for the transient and steady regimes (Bejan 1978; Poulikakos 1985). Also Poulikakos (1985) analyzes the importance of including the chemical species equation in order to predict the behavior of the fluid flow induced by thermal buoyancy. Solutions for the isotherms and streamlines were reported by Wesseling (1975) only for the steady state in terms of series expansions based on the Froude number (Fr) for a three-dimensional point-source and for a two-dimensional line-source.

On the other hand, other models describe convective phenomena by considering a horizontal circular cylinder buried in a porous medium and present numerical solutions for stream function and temperatures in a finite and discrete domain. Results have been given for the pure free convection case (Farouk and Shayer 1988) for half cylinder, due to the symmetrical characteristic of the phenomenon, and the combined convection case was solved (Badr and Pop 1988) for the whole cylinder by considering the combined convection on a non-dimensional approach based on the non-dimensional numbers of Grashhoff (Gr) and Reynolds (Re). The same problem was studied by Fernandez and Schrock (1982), who also found a correlation for Rayleigh (Ra) with the Nusselt number (Nu) which in turn is a function of the depth of the buried rod and an aspect ratio of the cylindrical source, the theory is also compared to their own experimental results.

An interesting work was presented by Kurdyumov and Liñán (2001). They developed a theory for an infinitesimal, horizontal source of heat embedded in an infinite porous medium. Unlike other models, three different scales were defined with an order of magnitude approach. There, numerical solutions for the streamlines and the isotherms for the natural convection case and the case when air streams are forced through the heat source at different angles of injection were reported. Kurdyumov and Liñán (2001) also extend the discussion of the theoretical and numerical work developed by Badr and Pop (1988), about the zones recirculation, under a forced convection scheme where the flow is induced vertically upward and

Table 1 Diagrammatic representation of the studies

Author	Study	Main result
Bejan (1978)	Theoretical approach of a punctual source of heat embedded in an infinite porous medium	Analytical solutions for the transient natural convection problem
Pouliakakos (1985)	Theoretical study of the buoyancy-driven heat and mass transfer flow induced by a point source of heat in an unbounded fluid-saturated porous medium	Development of a theory valid for small Rayleigh (Ra) numbers He analyzes the impact of species concentration gradients
Wesseling (1975)	Theoretical analysis of the buoyant plumes based on the Froude number (Fr) for a punctual line source of heat	Solutions for a two- to three-dimensional streamlines pattern
Farouk and Shayer (1988)	Numerical solution for natural convection for a heated cylinder embedded in a semi-infinite fluid-saturated porous medium	Due to the symmetry characteristic of the problem, numerical solutions for a half cylinder were developed
Badr and Pop (1988)	Numerical solutions for the combined convection for a cylindrical rod buried in a porous medium	Numerical results for the stream lines pattern at different Reynolds (Re) numbers at parallel flow and counter flow
Fernandez and Schrock (1982)	Experimental and numerical analysis for the natural convection for a buried cylinder embedded in a liquid-saturated porous medium	Numerical results for the isotherms and streamlines pattern, and a comparison with experimental data
Kurdyumov and Liñán (2001)	Theoretical and numerical analysis for the free and forced convection case for both, an infinitesimal source of heat and a cylindrical source buried in a saturated porous medium	Numerical results for the temperature field and the stream lines for the pure free convection case and the forced convection

downward, by analyzing the phenomenon at different air injection angles. All the previous cases are summarized in the diagram of Table 1.

From an experimental point of view, thermography has been used to visualize and measure isotherms in convective flows (Carlomagno and Cardone 2010; Luna et al. 2002; Medina et al. 2002; Astarita and Carlomagno 2013). The main limitation of this technique is that infrared thermography only gives information about the temperature distribution on surfaces. However, for convective two-dimensional flows the infrared thermography has been very useful to determine complex isotherms distributions.

Here, experiments using a digital infrared camera will be presented in the next section to prove the validity of the predictions for the buoyant plumes by Kurdyumov and Liñán (2001) where the isotherms pattern is generated around a small cylindrical source of heat made of a cylindrical electric resistance embedded in an air-saturated porous medium. Infrared visualization will be employed in § 3.1 to study the generation of the buoyant plumes under pure free convection conditions. In § 3.2 the buoyant plumes will be studied through the infrared thermography under a forced convection scheme due to the pass of constant air streams at different injection angles. The isotherms and their properties when the steady state is achieved, under free and forced convection, are analyzed quantitatively through the use of commercial software. Measurements were reported in terms of the characteristic scales proposed by Kurdyumov and Liñán (2001). In spite of some limitations, discussed later on, a good agreement between the predicted phenomena around the isotherms and the experimentally measured isotherms has been found. Conclusions will be given in § 3.

2 Experiments

2.1 Experimental setup

The buoyant plumes were generated by heating the surrounding medium with an electrical resistance that was placed inside of a cylindrical steel hollow rod, 0.009 m nominal diameter and 0.12 m nominal length, which was buried horizontally in an air-saturated porous medium. The porous medium was made of standard Ottawa sand, (850×10^{-6} m mesh, under ASTM C778 standard) which filled a black painted paperboard box (parallelepiped) 0.28 m height, 0.20 m length and 0.10 m depth, it will be advertised that close to the side walls, the porosity of the porous medium increases slightly with respect to the porosity in the core (Nield and Bejan 2013; Chen et al. 1996). This, rather than being a problem, enhances the mechanical contact among the grains and the paperboard, and improves the thermal contact itself. Hence, we have reproducibility in our measurements because several boxes filled with sand yield similar temperature

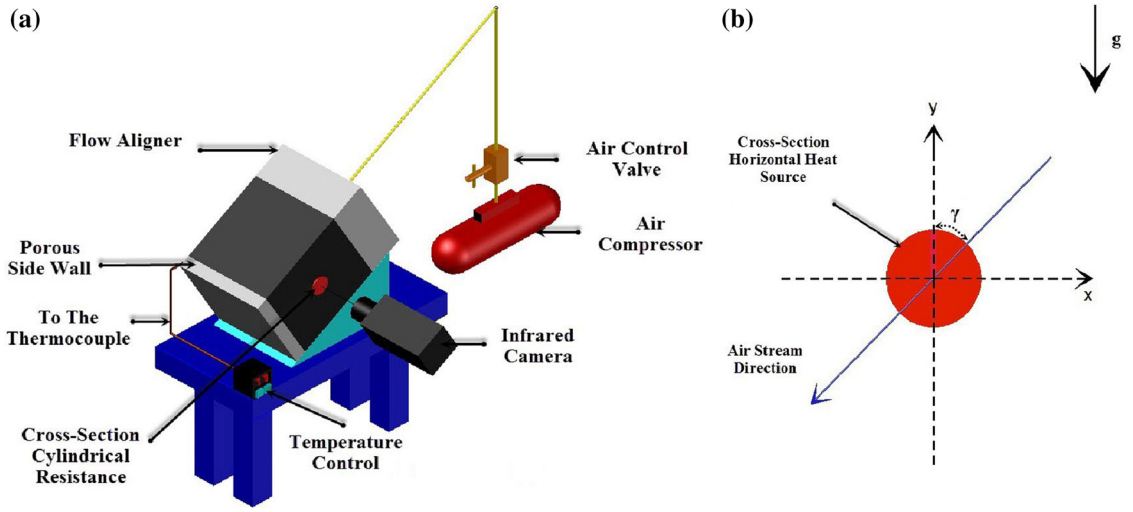

Fig. 1 **a** Experimental array, this scheme shows the case when the air stream has an angle γ referred to the vertical axis. **b** The coordinate system (x, y) always is maintained as is indicated

distributions. In order to set and control the temperature of the resistance at a constant value T_w, a type T thermocouple was placed at the rear end of the steel rod. This basic circuit was controlled with a West (6100+) process indicator. A nozzle connected to a compressor of 1.2×10^6 Pa was mounted together with a porous plastic foam as a flow aligner, the resulting circuit was placed on the right-hand side face of the paperboard box ensuring in this way an uniform and constant volume flow rate of air towards the porous medium, air emerges from the left-hand side porous side-wall. See Fig. 1, where the paperboard box is tilted with respect to the vertical axis at the angle γ.

To record the experiments, a digital infrared camera Flir (thermaCAM SC660) was used. The infrared camera has a measuring range that goes from 233.15 K to 1773.15 K, with a thermal sensitivity 30×10^{-3} K and a measurement error of 1.0%. The camera can also take temporal sequences of infrared pictures every 10 s with a resolution of 640×480 pixels (VGA quality) after an automatic self-calibration of camera. The infrared camera was placed at approximately 0.70 m from the frontal face of the paperboard box, and pointing towards to the center of it. All the set of experiments were carried out at room temperature T_∞ = 292 K and at atmospheric pressure.

2.2 Measurements

To capture all details of the isotherms, the infrared camera was programmed to take pictures every 10 s at a fixed temperature range that was preset at an interval between 298 and 323 K, the diffusion time (t_α) of the frontal paperboard box is estimated as follows $t_\alpha = \delta_p^2/\alpha_p \approx 8.196$ s where δ_p is the paperboard thickness and α_p is the paperboard diffusivity according to the diffusivity value reported by Sheng et al. (2002). The time t_α is the time of delay of any measurement of temperature on the face with respect to the inner region close to the paperboard. Data corresponding to the porous medium and the paperboard are given in Table 2. In agreement with Kurdyumov and Liñán model, heat intensity q, generated by the cylindrical resistance, is given by:

$$-q = \lambda \int_0^{2\pi} \frac{dT}{dr}\, r\, d\varphi\,, \tag{1}$$

where φ is the polar angle. The temperature field near the heat source was measured with the infrared camera, and a discrete formulation of Eq. (1) was used in order to calculate the heat flux supplied to the porous medium.

Because of the specific composition of a porous medium, conductive and convection phenomena can coexist in the same structure. The Rayleigh number (Ra) and the Nusselt number (Nu) are defined by Kurdyumov and Liñán (2001), respectively, as follows:

Table 2 General parameters used in the experiments

Property	Value
Permeability (K)	6×10^{-11} m^2
Porosity (ϕ)	0.650
Fluid density (Air at 293.15 K) (ρ_f)	1.2 kg/m^3
Fluid viscosity (Air at 293.15 K) (μ_f)	1.71×10^{-5} Pa s
Gravity acceleration (g)	9.810 m/s^2
Temperature of the heated cylinder (T_w)	353.15 K
Cylinder radius (a)	0.004795 m
Fluid coefficient of thermal expansion of air at 293 K (β)	0.003388 K^{-1}
Porous medium effective thermal diffusivity (α)	2.45×10^{-8} m^2/s
Effective conductivity (λ)	0.039 W/m[b]
Paperboard box thickness (d_p)	0.001 m
Paperboard diffusivity (α_p)	0.122×10^{-6} m^2/s[a]
Free stream velocity (V_∞)	3.78×10^{-4} m/s
Silica sand thermal conductivity (λ_s)	0.455 W/m K
Air conductivity (λ_{air})	0.026 W/m K
Heat intensity (q)	2.380 W/m

[a] Taken from (Sheng et al. 2002)
[b] Calculated with the correlation $\lambda = (1-\phi)\lambda_s + \phi\,\lambda_{\text{air}}$. (Nield and Bejan 2013)

$$Ra = \frac{K\rho_f \beta g (T_w - T_\infty) a}{\alpha \mu_f}\,, \tag{2}$$

$$Nu = \frac{q}{2\pi\lambda(T_w - T_\infty)}\,. \tag{3}$$

The Rayleigh number (Ra) associates the buoyancy with the convection, and on the other hand the Nusselt number (Nu) relates the heat transfer rate from the heat source to the permeable porous medium For all the set of experiments Ra is between 3.17×10^{-2} and 3.53×10^{-2} and $Nu \approx 0.160$. In order to standardize the experiment, three scales were also taken from Kurdyumov and Liñán (2001) as:

$$l_h = \frac{\mu_f\,\alpha\,\lambda}{K\,\rho_f\,g\,\beta\,q}\,, \tag{4}$$

$$v_h = \frac{K\rho_f \beta g q}{\mu_f \lambda}\,, \tag{5}$$

$$T_h - T_\infty = \frac{q}{\lambda}\,, \tag{6}$$

which correspond to a characteristic length, a characteristic velocity, and an a characteristic temperature rise above the ambient in the heated region around the source, respectively. Moreover, an expression for the non-dimensional temperature θ is given by:

$$\theta = \frac{T - T_\infty}{T_h - T_\infty}\,. \tag{7}$$

Meaning and values of the all parameters involved in the experiments are given in Table 2.

3 Experimental results

The main objective of the experiments is to observe the development of the buoyant plumes at different convective conditions and it is divided in two parts, for the first one the buoyant plumes are generated only by free convection conditions, i.e., the cylinder is only heated into the air-saturated porous medium. Is important to comment that no appreciable temperature gradients were observed on the lateral side-walls parallels to the pipe. It ensures that the temperature profiles around the cylindrical heat source are two-dimensional.

The second part was made to show the effects of the forced convection due to the action of a continuous air stream which will be directed at different tilt angles (γ) with respect to the vertical, for each single case of study through the porous medium, see Fig. 1b. According to the scales presented in § 2.2, the Péclet number is defined as follows:

$$Pe = \frac{l_h v_h}{\alpha} . \tag{8}$$

The Péclet number represents the ratio of advection to heat diffusion. This later non-dimensional parameter leads to order unity for the free convection case (advection and diffusion are of the same order). For the forced convection v_h is now substituted by the free stream velocity V_∞ which causes that the advection dominates over diffusion leading to a value of Péclet of $Pe \approx 59 \times 10^3$. The driven flows by a temperature gradient represent a basic model of thermal convection (Martynenko and Khramtsov 2005). The characteristic array of the buoyant plumes when the steady state is reached, under free and forced convection, results in well-defined zones of constant temperature in the vicinity of a plume, with respect to the next one. As a consequence of this configuration the temperature varies slightly, alongside the porous medium and as a result of this particular configuration the changes in density are also small as a function of the distance, under these conditions we can compare the experimental buoyant plumes with those numerically computed by Kurdyumov and Liñán (2001). Free and forced convection is useful to understand the changes in shape adopted by the buoyant plumes at different conditions. The quantitative analysis of the isotherms was made with the camera software Flir ResearchIR 2009.

3.1 Isotherms under free convection

We consider a cylinder of radius a embedded in an air-saturated porous medium at a temperature T_w which is higher than the surrounding medium T_∞.

In this configuration, the set of isotherms grow continuously until the steady state is reached (i.e., the time when the isotherms in the buoyant plumes do not change any more), as shown in squared brackets in Fig. 2 (snapshot 6). As it can be seen, the plume circularity is lost at short times (Fig. 2, snapshot 2) in comparison with the steady-state time, after which the plumes begin to adopt their characteristic ovoid shape. Figure 3 shows the temperature distribution along the vertical coordinate (y), and along the horizontal coordinate (x) that were made dimensionless according to the scales proposed by Kurdyumov and Liñán (2001), previously introduced in § 2.2.

3.2 Isotherms under combined free and forced convection

For the second part of the experiments, we considered the same heated cylindrical rod horizontally buried in the air-saturated porous medium at the conditions proposed in § 2.2. In this case, the convection is forced due to the existence of a constant air stream at angle γ (referred to the positive vertical axis y, measured clockwise, and by placing the origin at the center of the heat source) that is injected to have a non-dimensional velocity $U_\infty \approx 0.10$, this characteristic velocity value is taken from Kurdyumov and Liñán (2001). For our experimental purposes it is calculated as follows $U_\infty = V_\infty / v_h$ where V_∞ is the free stream velocity in m/s and is shown in Table 2. It is important to comment that the box and the camera were rotated simultaneously counter-clockwise, to attain the angle γ as is depicted in Fig. 1a. It allows to observe always the same spatial region and, thus, the air stream always is along an axis tilted with respect to the vertical at the angle γ.

In Fig. 4 the air stream flows at velocity $U_\infty = 0.10$, and it is forced downwards, at $\gamma = 0°$. The final shape adopted by the plume is strongly influenced by buoyant forces that dominate the phenomenon. In Fig. 5, the temperature distribution as a function of the distance is plotted with the infrared data obtained from Fig. 4. In Fig. 6 the air stream at velocity $U_\infty = 0.10$ is injected from the right-hand side wall of the paperboard box at an injection angle $\gamma = 90°$ in order to force the convection and achieve a buoyant plume. The non-symmetrical shape adopted by the buoyant plumes indicates that the intensity of the injected stream allows the buoyant forces to act on the porous medium domain, the infrared thermography agrees with the solutions proposed by Kurdyumov and Liñán (2001) for horizontally heated cylinders. In Fig. 7 the temperature distribution as a function of the distance is plotted with the infrared data obtained from Fig. 6.

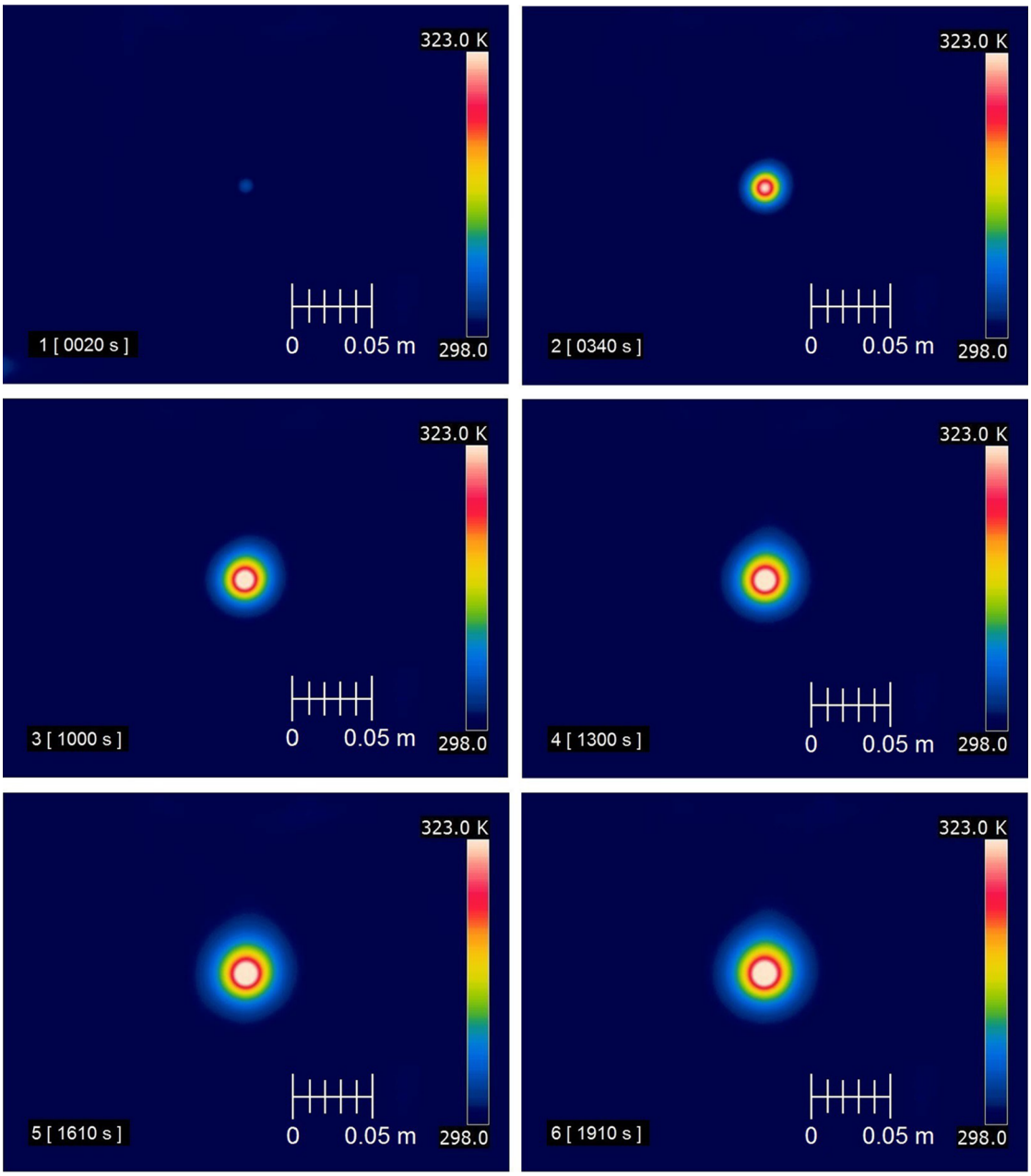

Fig. 2 Infrared snapshots showing the evolution of the buoyant plumes under pure free convection until stationary state is reached. The frame number is placed at the *left lower corner* of each *snapshot*, with its corresponding time scale (in seconds) in *square brackets*. The *color bar* on the *right-hand side* of every single *snapshot* gives the temperature scale. The spatial scale is also shown in each frame

At the last part of the experiments, the buoyant plumes were reached at different injection angles $\gamma = 30^\circ$, 45° and 60°. These injection angles are similar to those reported from the numerical computations for the line heat source problem proposed by Kurdyumov and Liñán (2001) except when $\gamma = 30^\circ$. The plumes show a strong dependence on its shape due to the several directions of the induced stream. According to the theory given by Kurdyumov and Liñán (2001) these plumes present recirculation in zones near the heat source as discussed in § 3.1. In Fig. 8, the corresponding infrared images for each injection angle γ are shown in snapshots 8a–c. Figure 8d shows the corresponding plots of the temperature distribution as a function of the distance taken along the direction of each injection angle $\gamma = 30^\circ$, $\gamma = 45^\circ$ and $\gamma = 60^\circ$.

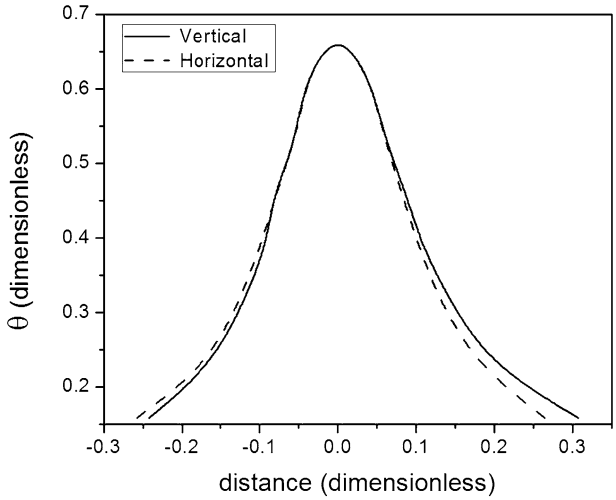

Fig. 3 Dimensionless plot showing the temperature distribution as a function of the distance. The *solid curve* is taken along the *vertical axis* centered at the middle of the heat source, and the *dashed curve* is taken along the *horizontal axis* centered at the heat source. This experimental plot was made from isotherms taken from Fig. 2 snapshot 6

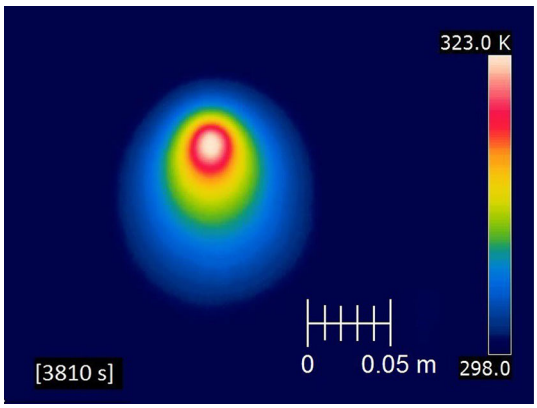

Fig. 4 Infrared image showing the buoyant plume due to forced convection induced from the upper wall of the air-saturated porous medium, the time scale when the steady state is reached (in seconds) is placed on the *left lower corner* in *square brackets*

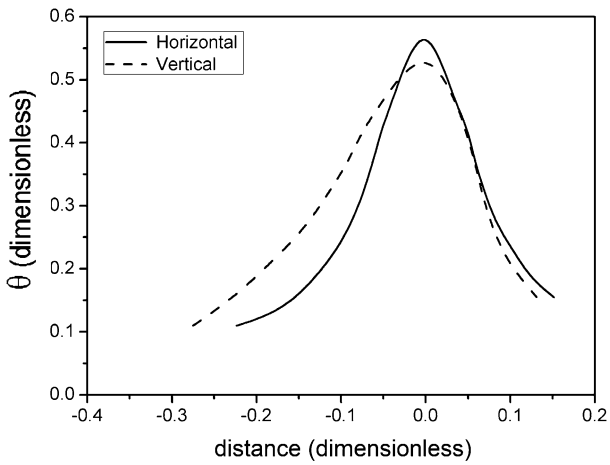

Fig. 5 Dimensionless plot showing the temperature distribution as a function of the distance. The *solid curve* is taken along the *horizontal axis* centered at the heat source, and the *dashed curve* is taken along the *vertical axis* centered at the heat source. This experimental plot was made from isotherms taken from Fig.4

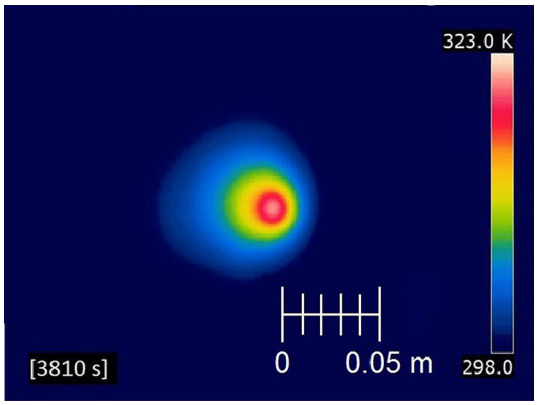

Fig. 6 Infrared image showing the buoyant plumes due to forced convection induced from the right wall of the air-saturated porous medium at $\gamma = 90°$, the time when the steady state is reached (in seconds) is placed on the *left lower corner* in *square brackets*

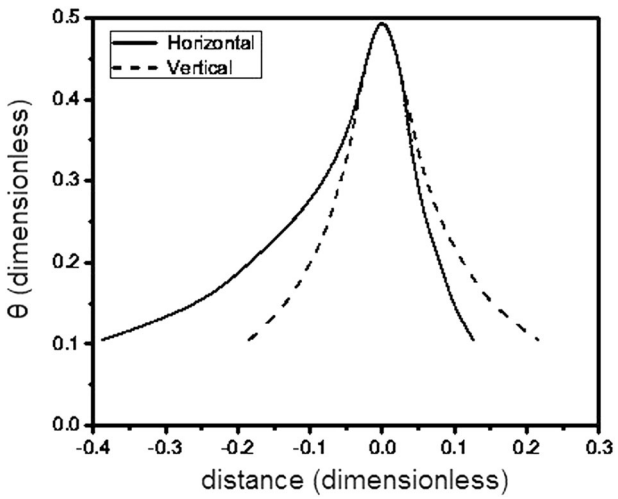

Fig. 7 Dimensionless plot showing the temperature distribution as a function of the distance. The *curve* plotted with a *solid line* is taken along the *horizontal axis* centered at the heat source, and the *curve* plotted with a *dashed line* is taken along the *vertical axis* centered at the heat source. This experimental plot was made from isotherms taken from Fig. 6

4 Conclusions

The buoyant plumes or isotherms around a heated source embedded in an air-saturated porous medium were visualized with an infrared camera and analyzed for the pure free convection case with digital thermography. These kinds of plumes were reproduced experimentally based on the theory developed by Kurdyumov and Liñán (2001). Digital infrared thermography allowed us to observe on the frontal face of a paperboard box of a paper box (with a delay) the overall evolution of the buoyant plumes until the steady state was reached. For the combined free and forced convection cases, when a continuous air stream is injected through the porous medium, different cases for the injection angle γ of the air stream were studied. Comparing the effects of the free and forced convection, the final shapes adopted by the buoyant plumes seem to be strongly affected by the action of the injection angle of the continuous air flow. It is apparent that this experimental study agrees very well with the theoretical predictions for the isotherms performed by Kurdyumov and Liñán (2001) who develop a global theory for the free and forced convection cases for the idealized case of an "horizontal line source of heat" and cylinders of radius a. The possible existence of recirculation zones was suggested by Kurdyumov and Liñán (2001) which can be characterized by plateaus in the temperature profiles as a function of y/l_h. However, our temperature measurements involve an error

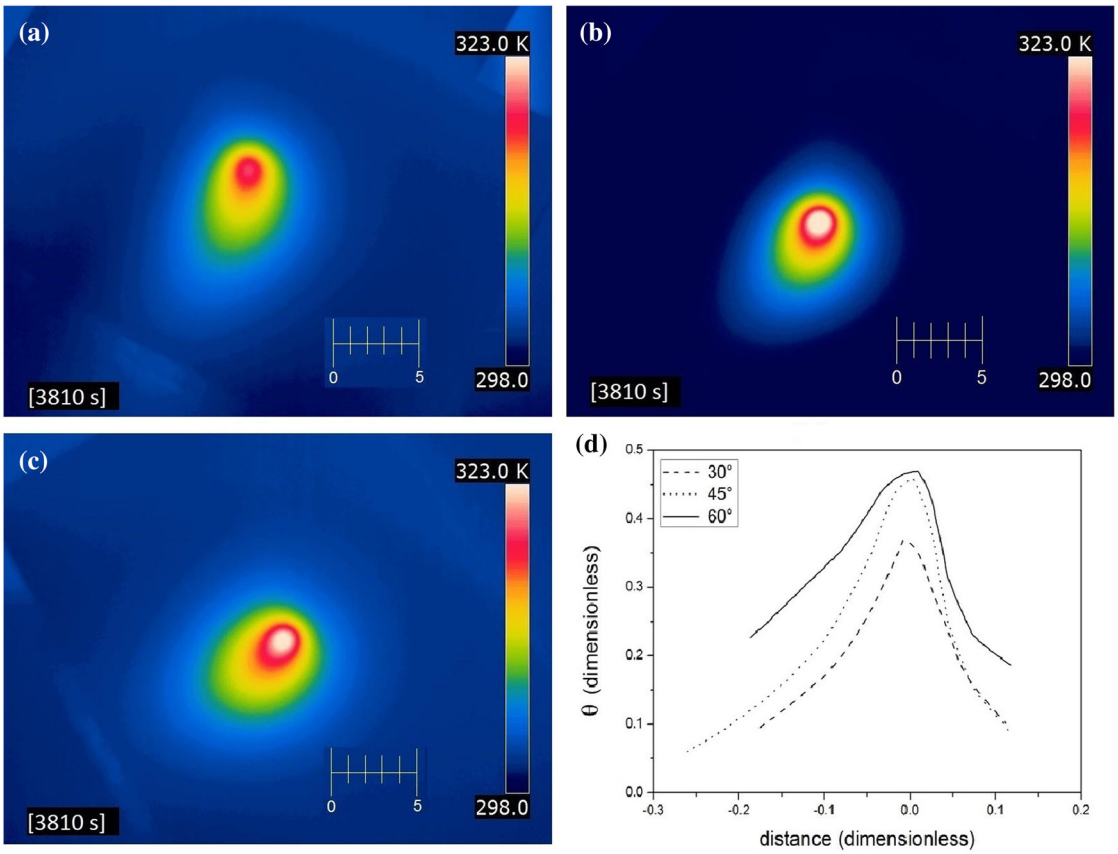

Fig. 8 Infrared images showing the buoyant plumes due to forced convection induced at different injection angles **a** $\gamma = 30°$, **b** $\gamma = 45°$ and **c** $\gamma = 60°$. The time to reach the steady state (in seconds) is placed on the *left lower corner* in the *square brackets* for each single snapshot. Picture **d** shows the corresponding plots of the temperature distribution as a function of the distance along the air stream direction at the angle γ

that does not allow us to confirm accurately or deny their existence. More precise studies must be made in order to discern about it. Our camera is not sensitive enough to achieve such a precision. Finally, this kind of studies could be useful, in problems related to many actual configurations in the oil industry, specifically in the so-called tertiary recovery methods as the steam assisted gravity drainage (SAGD) process in which it is important to control the oil flow direction towards the recovery well through a saturated porous medium. We consider that this process can be enhanced (by placing the extraction well at the most efficient positions) by controlling the distribution of isotherm and also by forcing the convection in the oil reservoir even after the steam flooding process.

Acknowledgments We are greatly indebted to Prof. Amable Liñán from E.T.S. Ingenieros Aeronáuticos, Universidad Politécnica de Madrid, for his unconditional support, helpful comments and suggestions for this experimental work. We wish also to thank to CONACYT, the Instituto Politécnico Nacional through the SIP-IPN 20160942 project, and the SENER-CONACYT project No. 147061 "Sistema Integral para la Generación de Vapor en Fondo de Pozo". Finally, we thank the anonymous reviewers of *Journal of Visualization* for their invaluable help in improving this work.

References

Astarita T, Carlomagno GM (2013) Infrared thermography for thermo-fluid-dynamics. Springer-Verlag, Berlin Heidelberg

Badr HM, Pop I (1988) Combined convection from an isothermal horizontal rod buried in a porous medium. Int J Heat and Mass Transfer 31:2527–2541

Bejan A (1978) Natural convection in an infinite porous medium with a concentrated heat source. J Fluid Mech 89:97–107

Carlomagno Giovanni Maria, Cardone Gennaro (2010) Infrared thermography for convective heat transfer measurements. Exp Fluids 49:1187–1218

Chen CH, Chen TS, Chen CK (1996) Non-Darcy mixed convection along non-isothermal vertical surfaces in porous media. Int J Heat Mass Transfer 39:1157–1164
Farouk B, Shayer H (1988) Natural convection around a heated cylinder in a saturated porous medium. J Heat Transfer 110:642–648
Fernandez RT, Schrock VE (1982) Natural Convection from cylinders buried in a liquid-saturated porous medium. Heat Transfer Proceedings of the International Heat Transfer Conference, 335–340
Kurdyumov VN, Liñán A (2001) Free and forced convection around line sources of heat and heated cylinders in porous media. J Fluid Mech 427:389–409
Luna E, Córdova A, Medina A, Higuera FJ (2002) Convection in a finite tilted fracture in a rock. Phys Lett A 300:449–455
Martynenko OG, Khramtsov PP (2005) Free convective heat transfer. Springer-Verlag, Berlin Heidelberg Berlin Heidelberg
Medina A, Luna E, Pérez-Rosales C, Higuera FJ (2002) Thermal convection in tilted porous fractures. J Phys Condens Mater 14:2467–2474
Nield D, Bejan A (2013) Convection in porous media. 1–5. Springer, New York
Poulikakos D (1985) On buoyancy induced heat and mass transfer from a concentrated source in an infinite porous medium. Int J Heat Mass Transfer 28:621–629
Sheng CK, Yunus M, Mahmood W (2002) Thermal diffusivity measurement of the commercial papers using photoacoustic technique. Pertanika J Sci & Technol 10(2):161–166
Wesseling P (1975) An asymptotic solution for slightly buoyant laminar plumes. J Fluid Mech 70:81–87